Mon. Not. R. Astron. Soc. **309**, L7–L11 (1999)

# Polarization light curves and position angle variation of beamed gamma-ray bursts

Gabriele Ghisellini[1★] and Davide Lazzati[1,2★]

[1]*Osservatorio Astronomico di Brera, Via Bianchi 46, I-23807 Merate (Lc), Italy*
[2]*Dipartimento di Fisica, Università degli Studi di Milano, Via Celoria 16, I-20133 Milano, Italy*

Accepted 1999 August 18. Received 1999 June 30

Downloaded from https://academic.oup.com/mnras/article/309/1/L7/1157854 by guest on 25 April 2024

**ABSTRACT**

The recently detected linear polarization in the optical light curve of GRB 990510 renewed interest in how polarization can be produced in gamma-ray burst fireballs. Here we present a model based on the assumption that we are seeing a collimated fireball, observed slightly off-axis. This introduces some degree of anisotropy, and makes it possible to observe a linearly polarized flux even if the magnetic field is completely tangled in the plane orthogonal to the line of sight. We construct the light curve of the polarization flux, showing that it is always characterized by two maxima, with the polarization position angle changing by 90° between the first and the second maximum. The very same geometry as assumed here implies that the total flux initially decays in time as a power law, but gradually steepens as the bulk Lorentz factor of the fireball decreases.

**Key words:** polarization – radiation mechanisms: non-thermal – gamma-rays: bursts.

## 1 INTRODUCTION

It is now widely believed that the afterglow emission of gamma-ray bursts is due to the deceleration of the relativistic fireball in the circumburst matter (for reviews see Piran 1999 and Mészáros 1999). This produces a shock which accelerates electrons to random relativistic energies and probably enhances the magnetic field, leading to the production of synchrotron emission. If the magnetic field is completely tangled over the entire range of emission regions seen by the observer, the resulting synchrotron emission is unpolarized. On the other hand, a very high degree of linear polarization can be expected if a fraction of the magnetic field is well ordered, reaching 60–70 per cent in the case of a completely ordered field. Polarization values in the optical band in the range 3–30 per cent have indeed been observed in cosmic sources, like BL Lac objects and high-polarization quasars (see e.g. Angel & Stockman 1980; Impey & Tapia 1990), the radiation of which is believed to be produced by the synchrotron process. One therefore expects that in gamma-ray burst afterglows also, the emission is polarized, and attempts have been made to measure it. After an upper limit (2.3 per cent) was found for GRB 990123 (Hjorth et al. 1999), Covino et al. (1999) detected linear polarization in the afterglow of GRB 990510, at the small but significant level of $1.7 \pm 0.2$ per cent. This detection was then confirmed by Wijers et al. (1999), who detected similar polarization values 2 h and 1 d later.

On the theoretical side, Gruzinov & Waxman (1999, hereafter GW99) and Gruzinov (1999) predict values of around 10 per cent, significantly larger than observed. This estimate is based on the assumption that the overall emission reaching the observer is produced in a finite number $N \sim 50$ of causally disconnected regions, each of which is embedded in a completely ordered magnetic field. The predicted total polarization level is 60 per cent$/\sqrt{N}$, equal to $\sim 10$ per cent for $N \sim 50$. GW99 discuss how the coherence length of the magnetic field generated at the external shock front of a gamma-ray burst fireball grows with time. If, however, the magnetic field is generated at the collisionless shock front, which is extremely local, it is not clear why the magnetic field embedded in the newly swept-up matter should be linked to the field in the regions behind the shock.

An alternative magnetic field generation process (and hence geometry) has been discussed by Medvedev & Loeb (1999, hereafter ML99), who consider a magnetic field completely tangled in the plane of the shock front, but with a high degree of coherence in the orthogonal direction. In the case of a spherical fireball, this geometry produces no polarization unless part of the fireball emission is amplified and part is obscured, as is the case in interstellar scintillation. In this case, however, the resulting polarization can be much better observed at radio wavelengths, and should show a rapid and erratic change of position angle.

We here propose an alternative model, in which the magnetic field geometry is analogous to that of ML99,[1] but in a fireball that

★ E-mail: gabriele@merate.mi.astro.it (GG); lazzati@merate.mi.astro.it (DL)

[1] Note however, that the ML99 instability is not the only process that can be responsible for such a geometry: see e.g. Laing (1980, hereafter L80).

© 1999 RAS

is collimated in a cone and observed slightly off-axis. In this case the circular symmetry is broken and net polarization can be observed (see e.g. Hjorth et al. 1999; Covino et al. 1999; Wijers et al. 1999). Evidence for beaming of the fireball of GRB 990510 from the anomalous decay of the optical light curve has been discussed in many recent papers (Harrison et al. 1999; Israel et al. 1999; Stanek et al. 1999b).

The key assumption of our model is that the fireball is collimated in a cone, observed slightly off-axis. The key results that we obtain are the polarization light curve, its connection with the flux behaviour, and a characteristic change of 90° in the polarization angle, making the model very easy to test.

## 2 POLARIZATION LIGHT CURVE

### 2.1 Magnetic field configuration

Assume a slab of magnetized plasma, in which the configuration of the magnetic field is completely tangled if the slab is observed face-on, while having some some degree of alignment if the slab is observed edge-on. Such a field can be produced by compression in one direction of a volume of 3D tangled magnetic field (L80) or by Weibel instability (ML99). If the slab is observed edge-on, the radiation is therefore polarized at a level $P_0$, which depends on the degree of order of the field in the plane. At an angle $\theta$ from the normal of the slab, the degree of polarization can be expressed as, following L80,

$$\frac{P(\theta)}{P_0} = \frac{\sin^2\theta}{1+\cos^2\theta}. \tag{1}$$

If the emitting slab moves in the direction normal to its plane with a bulk Lorentz factor $\Gamma$, we have to take into account the relativistic aberration of photons. This effect causes photons emitted at $\theta' = \pi/2$ in the (primed) comoving frame $K'$ to be observed at $\theta \sim 1/\Gamma$ (see also ML99).

### 2.2 Polarization of beamed fireballs

We assume that in gamma-ray burst fireballs the emitting region is a slab expanding radially and relativistically, compressed along the direction of motion. We assume also that the fireball is collimated into a cone of semi-aperture angle $\theta_c$, and that the line of sight makes an angle $\theta_o$ with the jet axis (upper panel of Fig. 1). As long as $\Gamma > 1/(\theta_c - \theta_o)$, the observer receives photons from a circle of semi-aperture angle $1/\Gamma$ around $\theta_o$ (i.e. within the grey shaded area of Fig. 2). Consider the edge of this circle: radiation coming from each sector is highly polarized, with the electric field oscillating in the radial direction (see also ML99). As long as we observe the entire circle, the configuration is symmetrical, making the total polarization vanish. However, if the observer does not see part of the circle, some net polarization survives in the observed radiation. This happens if a beamed fireball is observed off-axis when $1/(\theta_c + \theta_o) < \Gamma < 1/(\theta_c - \theta_o)$.

The probability of observing a cone along its axis is vanishingly small, since it corresponds to a small solid angle; there is thus a higher probability of observing the collimated fireball off-axis. If the cone angle $\theta_c$ is small, the probability $p(\theta_o/\theta_c)$ is approximately distributed as

$$p\left(\frac{\theta_o}{\theta_c}\right) \propto \frac{\theta_o}{\theta_c}; \quad \langle\theta_o\rangle = \frac{2}{3}\theta_c, \tag{2}$$

where $\langle\theta_o\rangle$ is the average off-axis angle.

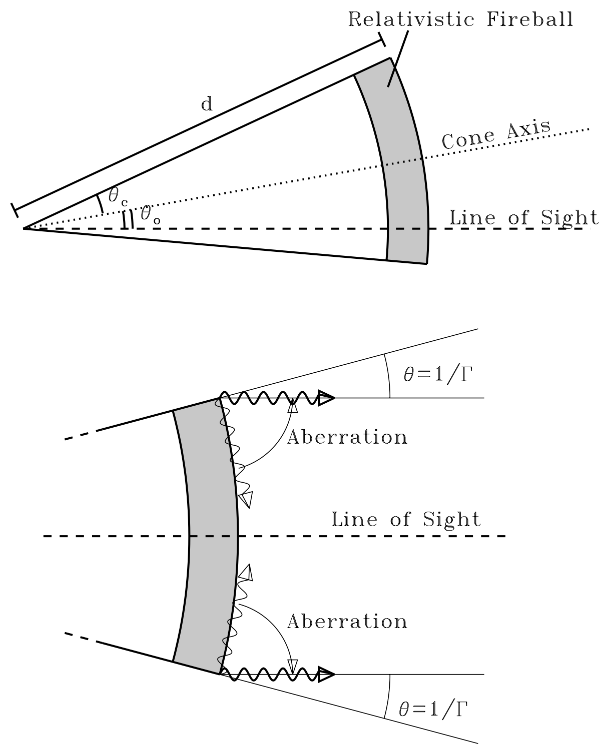


**Figure 1.** Geometry of the beamed fireball (upper panel). $\theta_o$ is the observer angle; $\theta_c$ is the cone aperture angle. The lower panel shows a close-up of the region around the line of sight. Note that the photons emitted in the comoving frame at an angle $\pi/2$ from the velocity vector are those making an angle $\theta \sim 1/\Gamma$ with the line of sight in the observer frame.

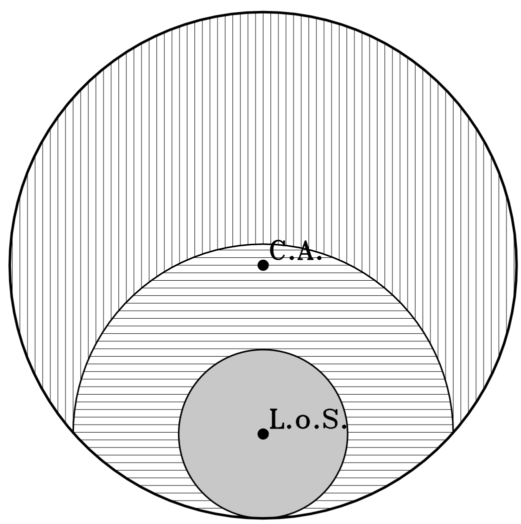


**Figure 2.** Front view of the beamed fireball, as in Fig. 1. C.A. stands for cone axis, while L.o.S. stands for line of sight. The grey shaded area produces unpolarized radiation, owing to the complete symmetry around the line of sight. The horizontally hatched region produces a horizontal component of polarization, while the upper region (vertically hatched) produces vertical polarization.

Assume therefore that $\theta_o/\theta_c > 0$ (Fig. 2). At the beginning of the afterglow, when $\Gamma$ is large, the observer sees only a small fraction of the fireball (grey shaded region in Fig. 2) and no polarization is observed. At later times, when $\Gamma$ becomes smaller



Downloaded from https://academic.oup.com/mnras/article/309/1/L7/1157854 by guest on 25 April 2024

than $1/(\theta_c - \theta_o)$, the observer will see only part of the circle centred on $\theta_o$; there is then an asymmetry, and a corresponding net polarization flux (horizontally hatched region of Fig. 2). To understand why the polarization angle in this configuration is horizontal, consider that the part of the circle that is not observed would have contributed to the polarization in the vertical direction. This missing fraction of vertical polarization does not cancel out the corresponding horizontal one, which therefore survives.

At later times, as the fireball slows down even more, a larger area becomes visible. When $\Gamma \sim 1/(\theta_c + \theta_o)$, the dominant contribution to the flux comes from the upper regions of the fireball (see Fig. 2), which are vertically polarized. The change of the position angle happens when the contributions from horizontal and vertical polarization are equal, resulting in a vanishing net polarization. At still later times, when $\Gamma \rightarrow 1$, light aberration vanishes, the observed magnetic field is completely tangled and the polarization disappears.

We therefore expect two maxima in the polarization light curve, the first for the horizontal component and the second for the vertical one.

The quantitative calculation of the light curve of the polarized fraction has been carried out as follows. We assume that the emission of each small volume of the fireball is isotropic in the comoving frame $K'$. We also assume that in this frame each small element emits the same instantaneous intensity. For each ring of radius $\rho$ and width $\mathrm{d}\rho$ of fireball material around the line of sight (see Fig. 3), the relativistically enhanced monochromatic intensity is computed as $I(\nu) = \delta^3 I'(\nu')$, where $\delta \equiv [\Gamma(1 - \beta\cos\theta)]^{-1}$ is the relativistic Doppler factor, and $\nu = \delta\nu'$. For $I'(\nu') \propto (\nu')^{-\alpha}$ we then have $I(\nu) = \delta^{3+\alpha} I'(\nu)$. Fig. 3 shows the geometrical set-up of the system. In our calculations, the distances $R$, $R_1$ and $\rho$ are considered as angles, since all of them scale with the distance $d$ of the fireball from the centre of explosion (see Fig. 1). In this case, $\rho$ is equivalent to the angle $\theta$ between the velocity vector of each element and the line of sight. Therefore the intensity observed from each element is a function of $\Gamma$ and $\rho$. The total intensity is obtained by integrating over the entire surface of the fireball, taking into account that each ring is observed at a different angle,

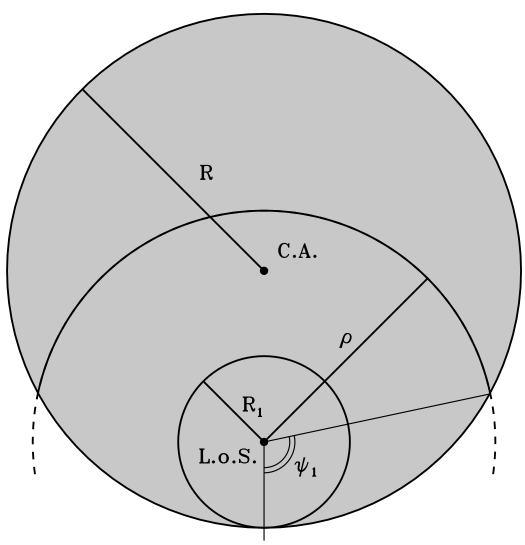


**Figure 3.** Sketch of the geometrical set-up used to compute the total and the polarized flux.

and then characterized by a different $\delta$. We assume a constant spectral index $\alpha = 0.6$ throughout our calculations. The total intensity from the entire fireball at a given time (and hence at a given $\Gamma$) is

$$I(\Gamma, \nu) = 2\pi \int_0^{R_1} I(\Gamma, \nu, \rho)\,\mathrm{d}\rho + \int_{R_1}^{2R-R_1} I(\Gamma, \nu, \rho)[2\pi - 2\psi_1(\rho)]\,\mathrm{d}\rho. \tag{3}$$

The first integral corresponds to the grey shaded area of Fig. 2, and to $\rho < R_1$ (see Fig. 3). The second integral corresponds to $\rho > R_1$. In this case we receive radiation only from a sector of the ring, between the angles $\psi_1$ and $2\pi - \psi_1$, with $\psi_1$ given by

$$\psi_1 = \frac{\pi}{2} - \arcsin\left[\frac{2R_1 R - R_1^2 - \rho^2}{2\rho(R - R_1)}\right]. \tag{4}$$

We now compute the polarized intensity. To this end, we consider again each element of the ring of radius $\rho$. After calculating the corresponding viewing angle in the comoving frame, we apply equation (1) to derive the intensity of the linearly polarized light. The position angle of the polarization produced by each element is in the radial direction. We then calculate the polarization of each ring by summing the polarization vectors. Finally, we integrate over $\rho$.

It is convenient to write the polarization vector as a complex number[2] $\boldsymbol{P}(\Gamma, \nu, \rho) \equiv P(\Gamma, \nu, \rho)\,\mathrm{e}^{2\mathrm{i}\theta_\mathrm{p}}$ and integrate it between $\psi_1$ and $2\pi - \psi_1$ (see Fig. 3). Here $\theta_\mathrm{p}$ is the position angle of the linear polarization in the observer frame. The polarization of a generic ring is

$$\boldsymbol{P}(\Gamma, \nu, \rho) = P(\Gamma, \nu, \rho) \int_{\psi_1}^{2\pi-\psi_1} \mathrm{e}^{2\mathrm{i}\psi}\,\mathrm{d}\psi = P(\Gamma, \nu, \rho)\sin(2\psi_1). \tag{5}$$

Since the result is a real number, the polarization direction can lie either in the plane that contains both the line of sight and the cone axis (we call this the 'vertical' polarization angle) or in the orthogonal plane (i.e. the 'horizontal' polarization angle). No intermediate values are possible.

Integration over $\rho$ then yields

$$\begin{aligned}\boldsymbol{P}(\Gamma, \nu) &= \frac{1}{I(\Gamma, \nu)} \int_{R_1}^{2R-R_1} I(\Gamma, \nu, \rho) P(\Gamma, \nu, \rho)\,\mathrm{d}\rho \int_{\psi_1}^{2\pi-\psi_1} \mathrm{e}^{2\mathrm{i}\psi}\,\mathrm{d}\psi \\ &= \frac{1}{I(\Gamma, \nu)} \int_{R_1}^{2R-R_1} I(\Gamma, \nu, \rho) P(\Gamma, \nu, \rho) \sin[2\psi_1(\rho)]\,\mathrm{d}\rho. \end{aligned} \tag{6}$$

For simplicity, we have neglected the light traveltime effects introduced by the overall curvature of the emitting regions (see Fig. 1), approximating the emitting volume with a slab. Since the degree of polarization of each element is divided by the total intensity of the same element, we expect these effects to be small in our case. Note that to include this effect requires us to assign a specific relationship between $\Gamma$ and the observed time $t$, which can be different for different models (e.g. adiabatic versus radiative evolution and/or gradients in the interstellar density).

The result of the numerical integration of equation (6) is shown in the lower panel of Fig. 4 for four different values of the off-axis ratio $\theta_o/\theta_c$. For the specific cases shown in the figure we have assumed $\theta_c = 5°$, but the general properties of the polarization light curve are unaffected by the particular choice of $\theta_c$. All the light curves (except the one with the lowest off-axis ratio, which

[2] This is fully equivalent to the Stokes notation of the $Q$ and $U$ parameters for linear polarization.



Downloaded from https://academic.oup.com/mnras/article/309/1/L7/1157854 by guest on 25 April 2024

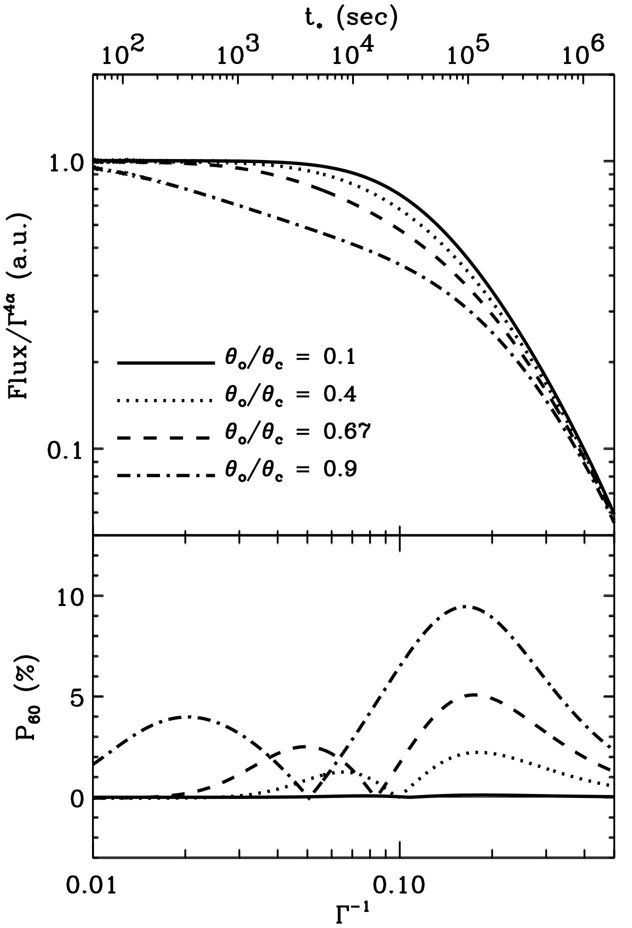


**Figure 4.** Light curves of the total flux (upper panel) and of the polarized fraction (bottom panel) for four different choices of the ratio $\theta_o/\theta_c$. The cone aperture angle $\theta_c = 5°$. $\theta_o$ is the viewing angle, as defined in Fig. 1. The higher the ratio $\theta_o/\theta_c$, the higher the polarized fraction owing to the increase of the asymmetry of the geometrical set-up. The actual value of the observed polarization depends linearly upon $P_0$ (see text). For this figure we have assumed $P_0 = 60$ per cent. The light curve of the total flux assumes a constant spectral index $\alpha = 0.6$ for the emitted radiation. Note that the highest polarization values are associated with total-flux light curves steepening more gradually. To calculate the value of time for upper $x$-axis ($t_*$), we have assumed $(t_*/t_0) = (\Gamma/\Gamma_0)^{-8/3}$ with $t_0 = 50$ s and $\Gamma_0 = 100$.

shows almost zero polarization) are characterized by two maxima in the polarized fraction. As discussed above, at the beginning the polarization is horizontal; it reaches a first maximum and then, when the polarized fraction vanishes, the angle abruptly changes by π/2. The polarized fraction rises again and then finally decreases to zero at late times. The second peak has a value that is always larger than the first one.

By interpolating the results of the numerical integrations (assuming $\alpha = 0.6$), we can express the maximum of the polarization light curve as a function of the off-axis angle:

$$P_{\max} \simeq 0.19 P_0 \left(\frac{\theta_o}{\theta_c}\right)^2 \left(\frac{1}{20} \leqslant \frac{\theta_o}{\theta_c} \leqslant 1; \quad 1° \leqslant \theta_c \leqslant 15°\right), \tag{7}$$

which is accurate within 5 per cent in the specified $\theta_o$ and $\theta_c$ ranges. This maximum always corresponds to the second peak.

## 3 LINK WITH THE TOTAL-FLUX LIGHT CURVE

The scenario proposed above for the polarization behaviour has a strict and direct link with the behaviour of the light curve of the total flux. The exact connection will depend on the specific model assumed for the deceleration of the fireball (i.e. homogeneous or radially distributed density of the interstellar medium, adiabatic or radiative regime, and so on), but there are general properties that can be incorporated in any model. For illustration, assume the simplest model of a spherical fireball expanding adiabatically in a homogeneous medium, predicting that the bulk Lorentz factor $\Gamma \propto t^{-3/8}$, and predicting a decay law for the flux density $F_\nu(t) \propto t^{-3\alpha/2}$ (Mészáros & Rees 1997), where $\alpha$ is the spectral index of the radiation spectrum, i.e. $F_\nu \propto \nu^{-\alpha}$. This law assumes that the flux is proportional to the source solid angle: if the fireball has reached a region of size $d$, then the accessible solid angle $\Omega \propto (d/\Gamma)^2 \propto (t\Gamma)^2 \propto t^{5/4}$. In the case of a fireball collimated in a cone of constant opening angle [e.g. neglecting for simplicity the possible lateral spreading of the fireball (Rhoads 1997, 1999; see see also Moderski, Sikora & Bulik 1999)], we will have the above relation as long as $1/\Gamma < \theta_c - \theta_o$. On the other hand, when $1/\Gamma$ becomes greater than $\theta_c + \theta_o$, all of the cone front becomes visible, and therefore $\Omega \propto (\theta_c d)^2 \propto (\theta_c t \Gamma^2)^2 \propto t^{1/2}$. This produces a steepening of the power-law light-curve decay, which now becomes $F_\nu(t) \propto t^{-3\alpha/2-3/4}$ (see also Mészáros & Rees 1999). At intermediate times, for which $\theta_c - \theta_o < 1/\Gamma < \theta_c + \theta_o$, the accessible solid angle increases with a law intermediate between $t^{5/4}$ and $t^{1/2}$, producing a *gradual* steepening in the light curve.

Assuming again $\Gamma \propto t^{-3/8}$, and calling $\Gamma_1 = 1/(\theta_c - \theta_o)$, $\Gamma_2 = 1/(\theta_c + \theta_o)$ and $t_1$, $t_2$ the corresponding times, we simply have

$$\frac{\Gamma_1}{\Gamma_2} = \left(\frac{t_2}{t_1}\right)^{3/8} \rightarrow \frac{\theta_o}{\theta_c} = \frac{(t_2/t_1)^{3/8} - 1}{(t_2/t_1)^{3/8} + 1}. \tag{8}$$

In the case of the GRB 990510 afterglow, the decay laws have been $t^{-0.9}$ at early times (Galama et al. 1999) up to ~ half a day after the burst event, and $t^{-2.5}$ after ~ 5 d (Israel et al. 1999). Therefore the ratio $t_2/t_1$ is of the order of 10–15, implying that $\theta_o/\theta_c$ is between 0.4 and 0.45. However, the observed steepening was larger than the value (3/4) derived above. Another cause of steepening can be the lateral spreading of the fireball, as suggested by Rhoads (1997), when $\Gamma \sim 1/\theta_c$ [but see Panaitescu & Mészáros (1999), who suggest that this phase should occur later]. In addition, some steepening of the light curve decay may be due to a curved synchrotron spectrum: in fact at early times the spectral index derived on the basis of *BVRI* photometric observations, dereddened with $E(B - V) = 0.20$, was flat ($\alpha = 0.61 \pm 0.12$, 21.5 h after the burst: Stanek et al. 1999b). Such a flat spectral index in the optical band must necessarily steepen at higher frequencies, to limit the emitted power. An estimate of such a steepening will come from the analysis of the X-ray afterglow flux, observed from 8 to 44.5 h after the burst (Kuulkers et al. 1999).

We conclude that the observed steepening of the light-curve decay may then be the combined result of a curved synchrotron spectrum and a collimated fireball. In this scenario, the spectral index of the late (after 5 d) optical spectrum should be $\alpha \sim 1.1$–1.2.



Downloaded from https://academic.oup.com/mnras/article/309/1/L7/1157854 by guest on 25 April 2024

## 4 DISCUSSION

We have proposed a model to derive the amount of linear polarization observable from a collimated fireball. We have shown that some degree of polarization can be observed even if the magnetic field is completely tangled in the plane of the fireball, as long as the fireball is observed slightly off-axis. One of the main virtues of the proposed model is its easily testable predictions: (i) the light curve of the degree of polarization has two maxima; (ii) the observable polarization position angles are fixed between the first and the second maximum, being orthogonal to each other; and (iii) there is a strong link with the light curve of the total flux.

The degree of polarization is predicted to be moderate, reaching 10 per cent only if we are observing a collimated fireball at its edge, and only for a short period of time. A larger degree of polarization would then suggest that the magnetic field is not completely tangled in the plane orthogonal to the line of sight, as suggested by GW99. Up to now very few attempts have been made to measure linear polarization in optical afterglows, and it is therefore premature to draw any firm conclusion from the upper limit detected in GRB 990123 (Hjorth et al. 1999) and from the positive detection in the case of GRB 990510 (Covino et al. 1999; Wijers et al. 1999). Note, however, that the light curve behaviour of GRB 990510 matches our predictions, as does the constant position angle of the observed polarization. At the time of the two first polarization measurements of GRB 990510 (made 2 h apart) the light curve of the total flux was decaying as $t^{-1.3}$ (Stanek et al. 1999a), i.e. it was already steepening, in agreement with our model. Unfortunately, the polarization value measured 1 d later (Wijers et al. 1999) was not precise enough to constrain the proposed scenario further.

It will be very interesting to explore in the future the association of a gradually steepening light curve and the presence of polarization. We cannot exclude the possibility that some of the already observed afterglows can indeed be fitted by steepening power laws, but the lack of data would make such an attempt meaningless. In addition, there are some optical afterglows (e.g. GRB 980326: Groot et al. 1998; GRB 980519: Halpern et al. 1999) that showed a rapid decay. In these cases we may have observed only that part of the light curve corresponding to $1/\Gamma > \theta_c + \theta_o$. From these considerations we conclude that GRB 990510 may not be unique in its category, and that a large fraction of gamma-ray burst afterglows can have some degree of optical linear polarization.

## REFERENCES

Angel J. R. P., Stockman H. S., 1980, ARA&A, 18, 321
Covino S. et al., 1999, A&A, 341, L1
Galama T. J. et al., 1999, GCN, 313
Groot P. J. et al., 1998, ApJ, 502, L123
Gruzinov A., 1999, ApJ, submitted (astro-ph/9905272)
Gruzinov A., Waxman E., 1999, ApJ, 511, 852(GW99)
Halpern J. P., Kemp J., Piran T., Bershady M. A., 1999, ApJ, 517, L105
Harrison F. A. et al., 1999, ApJ, submitted (astro-ph/9905306)
Hjorth J. et al., 1999, Sci, 283, 2073
Impey C. D., Tapia S., 1990, ApJ, 354, 124
Israel G. L. et al., 1999, A&A, 348, L5
Kuulkers E. et al., 1999, GCN, 326
Laing R. A., 1980, MNRAS, 193, 439 (L80)
Medvedev M. V., Loeb A., 1999, ApJ, in press (astro-ph/9904363) (ML99)
Mészáros P., 1999, Nucl. Phys. B, in press (astro-ph/9904038)
Mészáros P., Rees M. J., 1997, ApJ, 476, 232
Mészáros P., Rees M. J., 1999, MNRAS, 306, L39
Moderski R., Sikora M., Bulik T., 1999, ApJ, submitted (astro-ph/9904310)
Panaitescu A., Mészáros P., 1999, ApJ, submitted (astro-ph/9806016)
Piran T., 1999, Phys. Rep., in press, (astro-ph/9810256)
Rhoads J. E., 1997, ApJ, 487, L1
Rhoads J. E., 1999, ApJ, submitted (astro-ph/9903399)
Stanek K. Z., Garnavich P. M., Kaluzny J., Pych W., Thompson I., 1999a, GCN, 318
Stanek K. Z., Garnavich P. M., Kaluzny J., Pych W., Thompson I., 1999b, ApJ, 522, L39
Wijers R. A. M. J. et al., 1999, ApJ, in press (astro-ph/9906346)

This paper has been typeset from a TEX/LATEX file prepared by the author.

Downloaded from https://academic.oup.com/mnras/article/309/1/L7/1157854 by guest on 25 April 2024

© 1999 RAS, MNRAS **309**, L7–L11